

# Carbon Monoxide Oxidation over Au/Ce<sub>1-x</sub>Zr<sub>x</sub>O<sub>2</sub> Catalysts: Effects of Moisture Content in the Reactant Gas and Catalyst Pretreatment

Izabela Dobrosz-Gómez · Ireneusz Kocemba · Jacek M. Rynkowski

Received: 17 July 2008 / Accepted: 23 October 2008 / Published online: 11 November 2008  
© Springer Science+Business Media, LLC 2008

**Abstract** The Au/Ce<sub>1-x</sub>Zr<sub>x</sub>O<sub>2</sub> ( $x = 0, 0.25, 1$ ) catalysts were synthesized, characterized by BET, XRD, TPR-H<sub>2</sub>, HRTEM, AAS and tested in CO oxidation. The effect of moisture in the reactant gas on CO conversion has been studied in a wide range of concentrations (~0.7–6000 ppm). Moisture generates a positive effect on catalytic activity and wet conditions gave higher CO conversions. The optimum concentration of moisture for CO oxidation over Au/CeO<sub>2</sub> and Au/Ce<sub>0.75</sub>Zr<sub>0.25</sub>O<sub>2</sub> is 200–1000 ppm, while further increase in the moisture content suppresses CO conversion. The activity of the studied Au catalysts depends on the amount of moisture adsorbed on the catalyst rather than on its content in the feed stream, which suggests that the reaction involves water-derived species on the catalysts surface. The effect of the catalysts pretreatment in air, dry He, H<sub>2</sub> stream as well as H<sub>2</sub> + H<sub>2</sub>O gas mixture on their catalytic performance in CO oxidation has been also investigated. The model of the active sites for CO oxidation over the studied catalysts was proposed.

**Keywords** Au/Ce<sub>1-x</sub>Zr<sub>x</sub>O<sub>2</sub> catalyst · Au dispersion · CO oxidation · Moisture effect · Pretreatment effect

## 1 Introduction

It is well known that gold nanoparticles deposited on the metal-oxide supports exhibit a high catalytic activity in low

temperature CO oxidation [1]. Various parameters, including Au precursor, the size and shape of Au clusters, the nature of the support, the preparation method and the reaction conditions have already been considered as crucial factors influencing the catalytic activity of gold-containing systems [2–5]. Despite of many efforts in the investigation of supported Au catalysts for CO oxidation, the nature of active sites and the corresponding mechanism of this reaction remain under debate [6–8]. There have been several papers, sometimes contradictory, concerning the effect of the pretreatment conditions as well as the moisture content on the activity of supported Au catalysts in CO oxidation [9–12]. The increase in the oxidation activity in the presence of water was reported for Au/TiO<sub>2</sub> [9], Au/Fe<sub>2</sub>O<sub>3</sub> [4], Au/Al<sub>2</sub>O<sub>3</sub> [4, 10], Au/Mg(OH)<sub>2</sub> [11] catalysts obtained by a deposition-precipitation method. On the other hand, for an impregnated Au/TiO<sub>2</sub> catalyst [12] and Au/Ti(OH)<sub>4</sub>\*<sup>\*</sup>, derived from Au–phosphine complex precursor of Au and as-precipitated Ti(OH)<sub>4</sub>\*<sup>\*</sup> precursor of metal oxide support [13], the presence of water was found to suppress the catalytic activity. No effect was observed for Au/Fe(OH)<sub>3</sub>\*<sup>\*</sup> catalyst [13].

Previously, we reported the usefulness of CeO<sub>2</sub>–ZrO<sub>2</sub> mixed oxides, CeO<sub>2</sub> and ZrO<sub>2</sub> as supports for Au nanoparticles, mainly from the point of view their contribution to the reaction [14]. Considering that ceria-zirconia supported gold catalysts appeared to be very promising, the different factors controlling their structure and activity in CO oxidation were also presented [15]. Consequently, the main objective of this work is further investigation of Au/Ce<sub>1-x</sub>Zr<sub>x</sub>O<sub>2</sub> catalysts in dry and wet conditions. The high activity of the studied catalysts in the presence of moisture makes the catalysts advantageous for the potential applications at ambient conditions, especially in air purification systems and breathing apparatus. The industrial catalyst

I. Dobrosz-Gómez · I. Kocemba · J. M. Rynkowski  
Institute of General and Ecological Chemistry, Technical  
University of Łódź, Żeromskiego 116, 90-924 Łódź, Poland

I. Dobrosz-Gómez  
Facultad de Ciencias Exactas y Naturales, Universidad Nacional  
de Colombia, Sede Manizales, Colombia

used at present is hopcalite, a mixed oxide of copper and manganese ( $\text{CuMn}_2\text{O}_3$ ), which is susceptible to deactivation in the presence of water and is unsuitable for long term use [16]. On the other hand, fundamental studies are usually carried out under relatively dry conditions. Therefore, we believe that the study of the influence of moisture on the activity of Au catalysts in CO oxidation is worth of efforts. Also, a detailed insight into the effect of the catalysts pretreatment on their activity was gained, mostly from the point of view of the active sites for CO oxidation.

The  $\text{Au/Ce}_{1-x}\text{Zr}_x\text{O}_2$  ( $x = 0, 0.25, 1$ ) catalysts were synthesized, characterized by BET, XRD, TPR- $\text{H}_2$ , HRTEM, AAS and tested in CO oxidation. The influence of moisture in the reactant gas on CO conversion over  $\text{Au/CeO}_2$ ,  $\text{Au/ZrO}_2$  and  $\text{Au/Ce}_{0.75}\text{Zr}_{0.25}\text{O}_2$  catalysts has been quantitatively investigated over a wide range of concentrations ( $\sim 0.7$ –6000 ppm). The effect of the catalysts pretreatment in air, dry He,  $\text{H}_2$  stream as well as  $\text{H}_2 + \text{H}_2\text{O}$  gas mixture has been also studied.

## 2 Experimental

### 2.1 Synthesis

The oxide supports  $\text{CeO}_2$ ,  $\text{ZrO}_2$  and  $\text{Ce}_{0.75}\text{Zr}_{0.25}\text{O}_2$  solid solution were synthesized by the sol–gel like method, based on a thermal decomposition of mixed propionates, using as the starting materials, zirconium(IV) acetylacetonate [ $\text{Zr}(\text{CH}_3\text{COCH}_2\text{COCH}_3)_4$ , Avocado] and/or cerium (III) acetylacetonate hydrate [ $\text{Ce}(\text{CH}_3\text{COCH}_2\text{COCH}_3)_3 \cdot \text{H}_2\text{O}$ , Sigma-Aldrich] and calcined at  $550^\circ\text{C}$ , in details described previously [14].

The Au-based catalysts were prepared by the direct anionic exchange (DAE) method of gold species with hydroxyl groups of the support, using hydrogen tetrachloroaurate (III) trihydrate [ $\text{HAuCl}_4 \cdot 3\text{H}_2\text{O}$ , Sigma-Aldrich] as a precursor of the active gold phase, following the procedure describe previously [14]. In order to remove the residual chlorine from the catalysts, the obtained solids were suspended in 4 M ammonia solution, stirred 1 h and next centrifuged again. This washing agent is highly efficient (the amount of residual chlorine lower than 200 ppm) and greatly improves the dispersion of Au, preventing its agglomeration during the thermal treatment, as we presented previously [3, 15]. After drying in the oven at  $120^\circ\text{C}$  overnight, the samples were calcined in air at  $300^\circ\text{C}$  for 4 h. The nominal Au loading was 2 wt.%.

### 2.2 Characterization Methods

The specific surface area measurements ( $S_{\text{BET}}$ ) were performed by the BET method using  $\text{N}_2$  adsorption/desorption

at  $-196^\circ\text{C}$  (Sorptomatic 1900 apparatus; Carlo-Erba). Prior to the measurement, all samples were degassed for 4 h at  $250^\circ\text{C}$ .

Atomic Absorption Spectroscopy (AAS) analyses were performed with a Solaar M6 Unicam spectrophotometer in order to estimate the amount of Au deposited on supports, in details described previously [14].

High Resolution Transmission Electron Microscopy (HRTEM) measurements were carried out using high resolution microscopes EM-002B (TOPCON 200 kV) and JEOL-JEM 200CX at  $10^{-5}$  Pa to determine an average Au particle size and to define the gold particle size distribution more accurate, as described previously [3, 14]. Au particles are seen as the darker contrast on the oxide support surface.

X-ray diffraction (XRD) patterns were obtained at room temperature using a PANalytical X'Pert Pro MPD diffractometer, operating at 40 kV and 30 mA (Cu  $K_\alpha$  radiation). Data were collected in the range  $20$ – $70^\circ 2\theta$  with a step size of  $0.0167^\circ$  and step time of 10 s. JCPDS files were used for the identification of the diffraction peaks. The particle size ( $D_{\text{hkl}}$ ) was estimated using the Scherrer equation, as described previously [14].

Hydrogen Temperature Programmed Reduction ( $\text{H}_2$ -TPR) experiments were carried out by PEAK-4 apparatus, equipped with a thermal conductivity detector—TCD.  $\text{H}_2$ -TPR experiments were performed using a  $\text{H}_2/\text{Ar}$  (5 vol.%  $\text{H}_2$ , 95 vol.% Ar) gas mixture, with a flow rate of  $40\text{ cm}^3\text{ min}^{-1}$ , in the temperature range  $25$ – $850^\circ\text{C}$ , with a ramp rate  $15^\circ\text{C min}^{-1}$ . Powdered samples of 100 mg were exposed to dry Ar at  $250^\circ\text{C}$  for 1 h before the reduction. Based on the  $\text{H}_2$  formation, reduction degrees of the investigated samples were calculated, in details described previously [14].

CO oxidation reaction was carried out at atmospheric pressure in a quartz flow microreactor, provided with thermocouple, containing 100 mg of sample in a fixed bed, using a series of mass flow controllers with diluted gases. The gas mixture containing 1.6 vol.% CO, 3.3 vol.%  $\text{O}_2$  and 0.001 vol.%  $\text{H}_2\text{O}$  (He as an eluant gas) was used with a flow of  $50\text{ cm}^3\text{ min}^{-1}$ , in the temperature range  $25$ – $300^\circ\text{C}$ , with a ramp rate  $5^\circ\text{C min}^{-1}$ . The dry gas mixture ( $\sim 0.7$  ppm  $\text{H}_2\text{O}$ ) was obtained by passing the feed stream through the silica trap at dry ice–acetone temperature. Water vapour, when used, was introduced by passing the feed stream through a water saturator at room temperature and next through a freezer equipped with different freezing mixture (ice + water; ice + NaCl; ice +  $\text{H}_2\text{SO}_4$  66%). Thus, at 0,  $-14$ ,  $-20$  and  $-36^\circ\text{C}$ , the concentration of water vapour was 6000, 2000, 1000, and 200 ppm, respectively. Prior to the catalytic tests, the samples were heated in air stream at  $300^\circ\text{C}$  for 1 h with a ramp rate of  $5^\circ\text{C min}^{-1}$ , except for the pretreatment effect studies (the samples heated in: dry He, at 100, 200 and  $290^\circ\text{C}$ ;

H<sub>2</sub> (5.0 vol.)/Ar gas mixture at 200 and 290 °C; H<sub>2</sub> (5.0 vol.)/H<sub>2</sub>O (0.1 vol.)/Ar (94.9 vol.%) gas mixture at 200 °C). The reactant and product composition were analyzed on-line by a gas chromatograph equipped with a thermal conductivity detector, in which CO, O<sub>2</sub>, N<sub>2</sub> and H<sub>2</sub> were monitored. The catalytic experiments were repeated several times in order to verify their reproducibility.

### 3 Results and Discussion

#### 3.1 Characterization of Catalysts

The AAS analysis (Table 1) shows that the real amount of gold deposited on Ce-containing oxides and ZrO<sub>2</sub> is ca. 15 % and 30 % lower than the nominal Au loading (2 wt.%), respectively. According to our previous studies [14, 15], the real amount of Au deposited on the support surface during the anionic exchange process was almost identical to the nominal one, except for the Au/ZrO<sub>2</sub>, which presented the real Au loading ca. 20 % lower than the desired amount, due to the low specific surface area of zirconia. It confirms that the observed loss of Au in the case of the studied catalysts is attributed to the removal of non-attached gold complexes, simply adsorbed on the support surface due to the deficient quantity of hydroxyl groups available for anionic exchange, which takes place during the washing step. BET data show that the specific surface area of the catalysts is slightly lower or comparable to that of a given support (Table 1). The XRD pattern of CeO<sub>2</sub> (not presented here, in details discussed in our previous paper [14]) corresponds to a single cubic phase, fluorite-type structure (JCPDS: 03-065-2975) and that of ZrO<sub>2</sub> corresponds to both monoclinic (JCPDS: 00-037-1484) and tetragonal one (JCPDS: 00-050-1089). The diffraction analysis of Ce<sub>0.75</sub>Zr<sub>0.25</sub>O<sub>2</sub> confirms that the fluorite lattice structure has been preserved during the doping process.

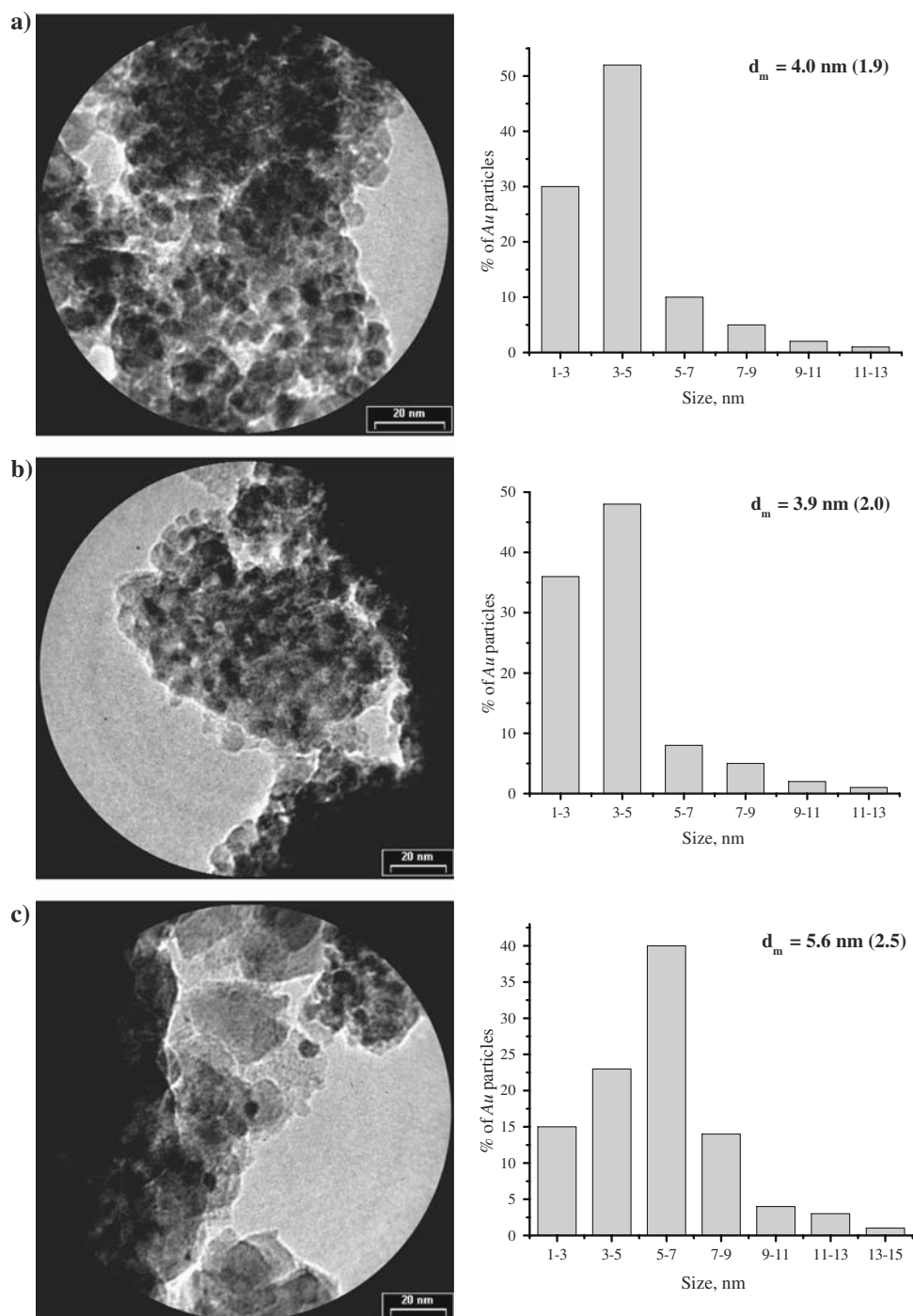
The position of the peaks is in accordance with the formation of a Ce<sub>0.75</sub>Zr<sub>0.25</sub>O<sub>2</sub> fluorite-structured solid solution (JCPDS: 00-028-0271), characterized by a face centred cubic cell (fcc) with  $a = 5.3490 \text{ \AA}$ , in comparison to  $a = 5.4112 \text{ \AA}$  calculated for pure CeO<sub>2</sub>. The lower ionic radius of Zr<sup>4+</sup> (0.84 Å compared to 0.97 Å for Ce<sup>4+</sup>) justifies the decrease of lattice parameters. Comparing to the XRD pattern of CeO<sub>2</sub>, the main diffraction peaks observed for the Ce<sub>0.75</sub>Zr<sub>0.25</sub>O<sub>2</sub> solid solution became broader. This broadening could be ascribed to the distortion of the cubic phase of fluorite structure due to the incorporation of ZrO<sub>2</sub>, resulting in the formation of smaller crystallites. The XRD patterns of Au/Ce<sub>1-x</sub>Zr<sub>x</sub>O<sub>2</sub> ( $x = 0; 0.25, 1$ ) catalysts are nearly identical to those of given supports. No clear Au reflections were observed in the XRD patterns of all studied catalysts, suggesting the presence of well dispersed small Au particles. However, a shift of the four main diffraction peaks corresponding to the (101) (110) (200) (211) reflections typical of a face-centered cubic (fcc) cell towards lower  $2\theta$  angles was observed. It could be related to the lattice expansion due to the formation of Ce<sup>3+</sup> cations, having a bigger radius than Ce<sup>4+</sup> (1.14 Å vs. 0.97 Å) [17], suggesting the “autoreduction” of the catalysts surface during the calcination process. In general, Au deposition does not have an influence on the crystallite size of the supports, except for Au/CeO<sub>2</sub> catalyst, which presents the crystallite size of CeO<sub>2</sub> twice lower than that of the support. The BET and XRD results present that the loading of ca. 2 wt.% Au does not modify the characteristic textural and morphological properties of the supports. The presence of spherical Au particles of different size is observed (Fig. 1). For Au supported on CeO<sub>2</sub> and Ce<sub>0.75</sub>Zr<sub>0.25</sub>O<sub>2</sub>, approximately 80% of Au particles are in the range of 1–5 nm, with the mean particle diameter of ca. 4 nm ( $\pm 2.0$ ). On the other hand, for Au/ZrO<sub>2</sub> catalyst only 40 % of Au particles are in this range, whereas the other 40 % are in the range of 1–7 nm.

**Table 1** Characterization data of Au/Ce<sub>1-x</sub>Zr<sub>x</sub>O<sub>2</sub> ( $x = 0, 0.25, 1$ ) catalysts and their oxide supports obtained using various physicochemical techniques

Sample denotation	Real Au loading <sup>a</sup> (wt.%)	Surface area <sup>b</sup> (m <sup>2</sup> g <sup>-1</sup> )	Lattice type and the average particle size <sup>c</sup> of oxide support (nm)	D <sub>Au</sub> <sup>d</sup> (nm)	H2-TPR data <sup>e</sup>			
					T <sub>0</sub> (°C)	T <sub>max peak I</sub> (°C)	T <sub>max peak II</sub> (°C)	Total H <sub>2</sub> consumption (mmol g <sup>-1</sup> )
Au/CeO <sub>2</sub>	1.79	51.5	Cubic Ce(111) 6.4	4.0	85	200	840	0.78
CeO <sub>2</sub>	–	58.1	Cubic Ce(111) 14.2	–	300	520	840	1.14
Au/Ce <sub>0.75</sub> Zr <sub>0.25</sub> O <sub>2</sub>	1.68	49.5	Cubic Ce(111) 7.2	3.9	50	200	750	0.95
Ce <sub>0.75</sub> Zr <sub>0.25</sub> O <sub>2</sub>	–	50.1	Cubic Ce(111) 7.0	–	290	565	740	1.53
Au/ZrO <sub>2</sub>	1.45	3.8	Monoclinic Zr(-111) 27.8 tetragonal Zr(101) 18.8	5.6	230	350	685	0.14
ZrO <sub>2</sub>	–	4.5	Monoclinic Zr(-111) 23.4 tetragonal Zr(101) 19.0	–	230	380	795	0.20

Determined by: <sup>a</sup> AAS, <sup>b</sup> N2-BET, <sup>c</sup> XRD, <sup>d</sup> HRTEM DAu—average diameter of Au particles, <sup>e</sup> H2-TPR

**Fig. 1** HRTEM images together and histograms of Au particle size distribution on **a**  $\text{CeO}_2$ , **b**  $\text{Ce}_{0.75}\text{Zr}_{0.25}\text{O}_2$  and **c**  $\text{ZrO}_2$



The Au particles larger than 7 nm are also present, especially in the case of  $\text{Au}/\text{ZrO}_2$  catalyst. The mean particle diameter for  $\text{Au}/\text{ZrO}_2$  is ca. 5.6 nm ( $\pm 2.5$ ). The formation of the larger Au agglomerates is enhanced by low specific surface area of  $\text{ZrO}_2$ .

Figure 2 presents  $\text{H}_2$ -TPR profiles of  $\text{Au}/\text{Ce}_{1-x}\text{Zr}_x\text{O}_2$  ( $x = 0, 0.25, 1$ ) catalysts (continuous lines) and the corresponding oxide supports (broken lines). Reduction of  $\text{CeO}_2$  occurs in two stages with maxima at 520 °C, which can be

ascribed to the reduction of the most easily reducible surface capping oxygen and 840 °C reflecting bulk reduction of  $\text{CeO}_2$  and the creation of lower cerium oxides [18–20]. Beside the low temperature peak, a characteristic shoulder at 450 °C is observed which could be related to the possibility of the formation of intermediate phases as the origin of the low temperature peak of  $\text{CeO}_2$  reduction [21]. It indicates that there are at least two types of  $\text{Ce}^{4+}$  located at different chemical environments, assigned to the reduction



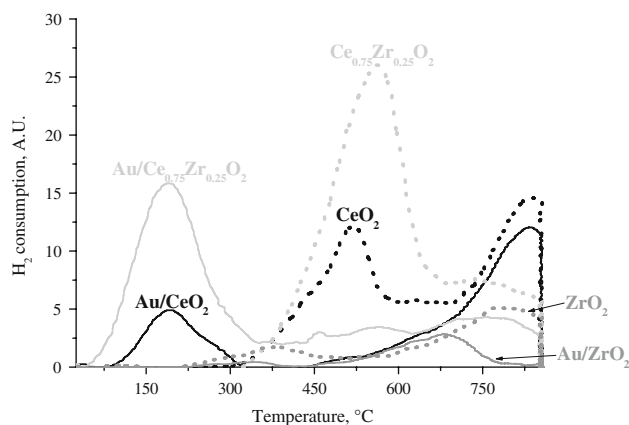


**Fig. 2** H<sub>2</sub>-TPR profiles of Au/Ce<sub>1-x</sub>Zr<sub>x</sub>O<sub>2</sub> ( $x = 0, 0.25, 1$ ) catalysts and their oxide supports

of surface and subsurface Ce<sup>4+</sup>, as previously observed by He et al. [22]. The incorporation of ZrO<sub>2</sub> into CeO<sub>2</sub> gives the material in which reducibility features like relative intensity and the position of peaks are different: the peak present at 520 °C for CeO<sub>2</sub> becomes larger and, on the other hand, that at 840 °C becomes smaller. A shift of the maximum of the low temperature reduction peak towards higher temperature is also observed. Moreover, for Ce<sub>0.75</sub>Zr<sub>0.25</sub>O<sub>2</sub> mixed oxide, the H<sub>2</sub> consumption starts at slightly lower temperature than for ceria. This special behaviour could be related to the phase distortion, which would alternatively shorten or lengthen the metal-oxygen bonds. Furthermore, the lengthening of the metal-oxygen bond would result in a lower barrier of energy for the oxygen migration in the bulk. On the other hand, ZrO<sub>2</sub> is considered to be a non-reducible oxide. However, some authors [23] reported negligible hydrogen consumption during ZrO<sub>2</sub> reduction. The results of presented study confirm some reducibility of zirconia, especially at higher temperature with the maximum at around 800 °C. However, it must be noted that ZrO<sub>2</sub> is much more resistant to the reduction, comparing to CeO<sub>2</sub> and Ce<sub>0.75</sub>Zr<sub>0.25</sub>O<sub>2</sub> mixed oxide.

H<sub>2</sub>-TPR measurements show a significant effect of the Au particles on reducibility of the oxide supports. One can see that the deposition of small Au nanoparticles leads to a decrease in the temperature at which reduction occurs. The reduction of Au/CeO<sub>2</sub> catalyst occurs in two stages with maxima at 200 °C, which can be ascribed to the reduction of oxygen species coordinated around finely dispersed Au particles and the ceria surface layers and 840 °C reflecting bulk reduction of CeO<sub>2</sub> accompanied by the formation of non-stoichiometric cerium oxides. The H<sub>2</sub>-TPR profile of Au/ZrO<sub>2</sub> catalyst consists of two peaks slightly shifted to lower temperatures, comparing to ZrO<sub>2</sub>. Similarly to Au/CeO<sub>2</sub>, the presence of Au on Ce<sub>0.75</sub>Zr<sub>0.25</sub>O<sub>2</sub> mixed oxide effectively promotes the reduction of its surface, as confirmed by a characteristic shift of its low-temperature

reduction peak towards lower temperature. The observed characteristic decrease in the reduction temperature of Au/CeO<sub>2</sub> and Au/Ce<sub>0.75</sub>Zr<sub>0.25</sub>O<sub>2</sub> catalysts as compared with oxide supports, suggests that the presence of well-dispersed Au nanoparticles facilitates activation (dissociation) of hydrogen molecule on metallic gold particles and leads to the migration of the dissociated hydrogen species by a spill-over process from the Au particles to the support surface. However, if the catalyst contains only ionic gold, the surface oxygen reducibility could be intensified through the lattice substitution mechanism, as reported by Fu et al. [24]. According to those statements, the Au<sup>+</sup> or Au<sup>3+</sup> ions would fill the vacant Ce<sup>4+</sup> sites resulting in the oxygen vacancies formation and the increase in oxygen mobility and reducibility. In this case, the presence of gold causes a decrease in the strength of the surface Ce-O bonds adjacent to gold atoms, thus leading to higher surface lattice oxygen mobility [25]. It should be also noted that for Au/Ce<sub>0.75</sub>Zr<sub>0.25</sub>O<sub>2</sub> catalyst, the H<sub>2</sub> consumption starts at a lower temperature than for Au/CeO<sub>2</sub>.

The addition of Au causes also a considerable decrease in H<sub>2</sub>-TPR signal intensity, especially visible for Ce-containing samples (Fig. 2). One can see that the amount of H<sub>2</sub> used for the reduction of the studied catalysts is lower than that observed for the respective supports (Table 1). Notably, the H<sub>2</sub> uptake for Au/CeO<sub>2</sub> (0.17 mmol g<sup>-1</sup>) and Au/Ce<sub>0.75</sub>Zr<sub>0.25</sub>O<sub>2</sub> (0.55 mmol.g<sup>-1</sup>) catalysts estimated on the basis of low temperature reduction peak is always higher than the amount required for the reduction of the metal precursor. This indicates that the reduction of surface Ce<sup>4+</sup> also occurs. It should be also noted that the amount of H<sub>2</sub> used for the reduction of calcined Au/Ce<sub>0.75</sub>Zr<sub>0.25</sub>O<sub>2</sub> (0.95 mmol.g<sup>-1</sup>) catalyst is lower than that observed for both uncalcined (dried) Au/Ce<sub>0.75</sub>Zr<sub>0.25</sub>O<sub>2</sub> catalyst precursor (1.12 mmol g<sup>-1</sup>) and support oxide Ce<sub>0.75</sub>Zr<sub>0.25</sub>O<sub>2</sub> (1.53 mmol g<sup>-1</sup>). Moreover, the H<sub>2</sub> uptake estimated basing on of the low-temperature reduction peak for calcined Au/Ce<sub>0.75</sub>Zr<sub>0.25</sub>O<sub>2</sub> catalyst (0.55 mmol g<sup>-1</sup>) is lower than that for the uncalcined catalyst precursor (0.64 mmol g<sup>-1</sup>), confirming the catalyst “autoreduction” during the calcination process. The “autoreduction” phenomenon is probably the reason for the change in the catalysts colour during drying and calcination processes from yellow to dark grey and from dark grey to graphite, respectively. It can also explain the characteristic shift of main diffraction peaks in the XRD pattern of supported Au catalysts. Moreover, the amount of H<sub>2</sub> used for the reduction of the studied catalysts strongly depends on the oxide support composition, with the highest H<sub>2</sub> consumption observed for Au/Ce<sub>0.75</sub>Zr<sub>0.25</sub>O<sub>2</sub> (Table 1). In the case of supports, the H<sub>2</sub> consumption was also higher for Ce<sub>0.75</sub>Zr<sub>0.25</sub>O<sub>2</sub> than that observed for CeO<sub>2</sub>. According to XRD studies, both oxide supports were characterized by a single cubic phase, fluorite-type

structure. However, for  $\text{Ce}_{0.75}\text{Zr}_{0.25}\text{O}_2$  it was observed that the substitution of  $\text{Ce}^{4+}$  cation with the smaller  $\text{Zr}^{4+}$  one causes lowering of symmetry and a decrease in unit cell parameters. Moreover, comparing to the XRD pattern of  $\text{CeO}_2$ , the main diffraction peaks observed for  $\text{Ce}_{0.75}\text{Zr}_{0.25}\text{O}_2$  mixed oxide became broader. This broadening was ascribed to the distortion of the cubic phase due to  $\text{ZrO}_2$  incorporation. It suggests that the presence of such structural modifications leads to the increase in the quantity of oxygen available at lower temperature, as proposed by Trovarelli et al. [26].

## 3.2 Catalytic Activity in CO Oxidation

### 3.2.1 Effect of Moisture Content

Figure 3 presents a series of curves showing the effect of the reaction temperature on the CO conversion over  $\text{Au/CeO}_2$ ,  $\text{Au/Ce}_{0.75}\text{Zr}_{0.25}\text{O}_2$  and  $\text{Au/ZrO}_2$  catalysts, in dry and moisturized  $\text{CO/O}_2$  gas mixture. Typical smooth light-off behaviour is observed and CO conversion increases slightly with temperature. However, the strong dependence of the CO conversion on the moisture concentration is observed.

It is noted that at  $\sim 0.7$  ppm  $\text{H}_2\text{O}$ , CO conversion over  $\text{Au/CeO}_2$  and  $\text{Au/Ce}_{0.75}\text{Zr}_{0.25}\text{O}_2$  is lower ca. 2 orders of magnitude than that under usual reactant conditions (10 ppm  $\text{H}_2\text{O}$ ). However, no marked difference in CO conversion at  $\sim 0.7$  and 10 ppm  $\text{H}_2\text{O}$  over  $\text{Au/ZrO}_2$  catalyst was observed. The presence of moisture generates a positive effect on catalytic activity in CO oxidation and wet conditions gave higher CO conversions. One can see that CO conversion over  $\text{Au/CeO}_2$  and  $\text{Au/Ce}_{0.75}\text{Zr}_{0.25}\text{O}_2$  increases with the increase in moisture content, reaches a maximum in the range of 200–1000 ppm  $\text{H}_2\text{O}$ . Suppression of the reaction by the excess amount of water can be explained by blocking of the catalytic active sites, as proposed by Daté et Haruta for  $\text{Au/TiO}_2$  [9] or competitive adsorption of moisture and  $\text{O}_2$ . On the other hand, a continuous augmentation of CO conversion over  $\text{Au/ZrO}_2$  catalyst with the increase in the moisture content is observed. However, only the addition of considerable amount of moisture ( $>1000$  ppm  $\text{H}_2\text{O}$ ) leads to such significant increase in CO conversion.

As presented in Fig. 4, the effect of moisture on CO oxidation rate over three studied catalysts is different. The highest activity was obtained over  $\text{Au/Ce}_{0.75}\text{Zr}_{0.25}\text{O}_2$

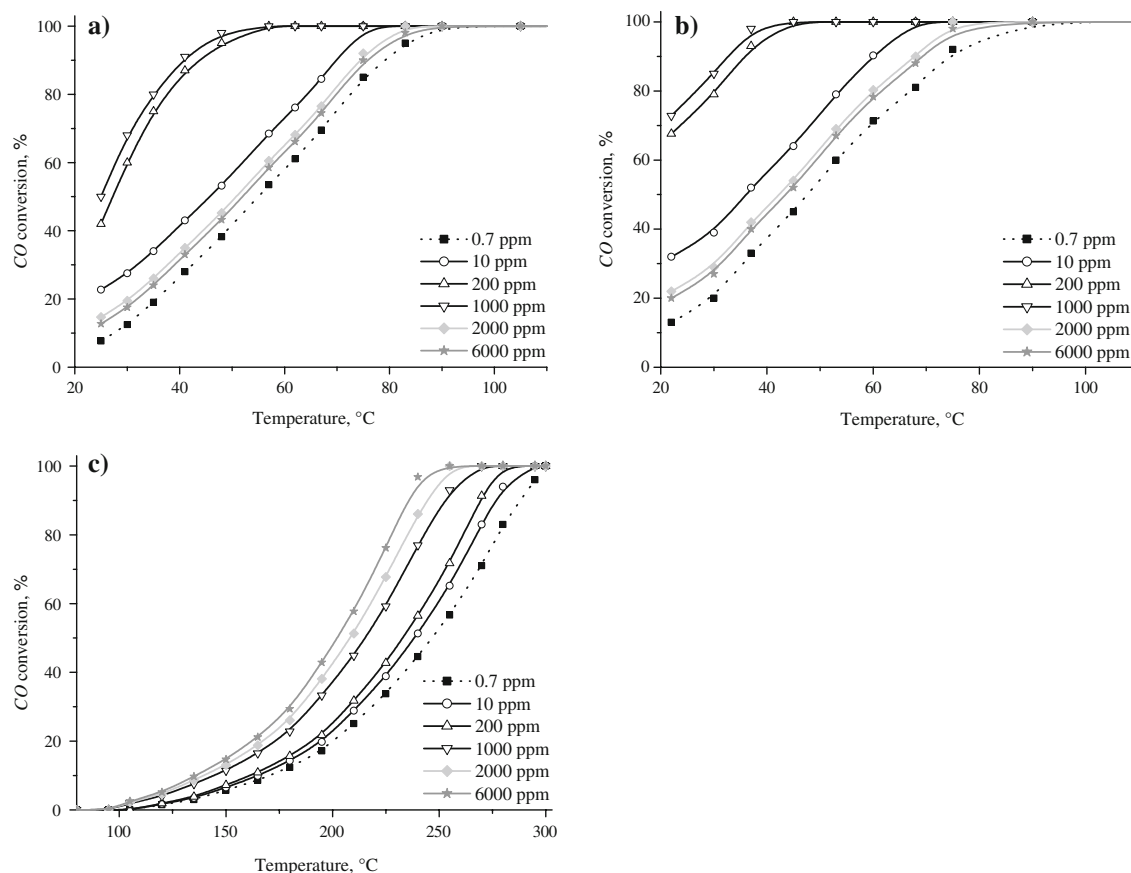


**Fig. 3** CO conversion as a function of the reaction temperature in the presence of different moisture concentration over **a**  $\text{Au/CeO}_2$ , **b**  $\text{Au/Ce}_{0.75}\text{Zr}_{0.25}\text{O}_2$ , **c**  $\text{Au/ZrO}_2$  ( $\text{CO}:\text{O}_2:\text{He} = 1.7:3.4:\text{balance}$ ;  $\text{W/F} = 0.12 \text{ g s cm}^{-3}$ )

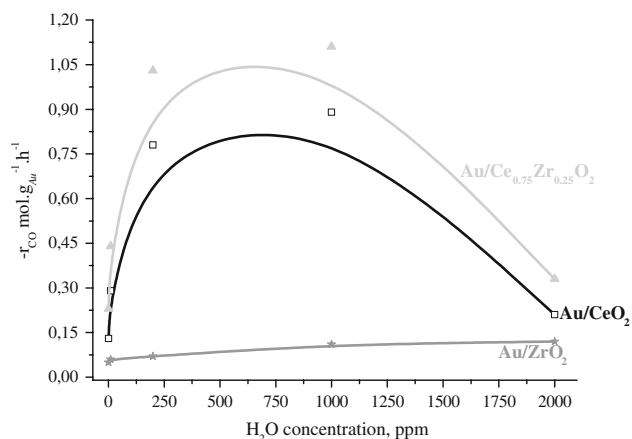


**Fig. 4** Dependence of the CO oxidation reaction rate at 30 °C over Au/CeO<sub>2</sub> and Au/Ce<sub>0.75</sub>Zr<sub>0.25</sub>O<sub>2</sub> and at 150 °C over Au/ZrO<sub>2</sub> in the presence of different moisture concentration (CO:O<sub>2</sub>:He = 1.7:3.4:balance; W/F = 0.12 g s cm<sup>-3</sup>)

catalyst and the lowest over Au/ZrO<sub>2</sub> one. It suggests that both the reaction mechanism and the different behaviour of the studied catalysts in the presence and absence of water strongly depend on the nature of the support. Independent of the moisture content, the activity of the studied catalysts was following the order: Au/ZrO<sub>2</sub> < Au/CeO<sub>2</sub> < Au/Ce<sub>0.75</sub>Zr<sub>0.25</sub>O<sub>2</sub>. One can see that the sequence of the decreasing temperature of catalysts reduction (Table 1) is followed by the sequence of the increasing activity. Thus, in the presence of highly dispersed Au nanoparticles, ceria-containing support is susceptible to the reduction at lower temperature and appears to be responsible for the activity of studied catalysts. For this reason Au nanoparticles deposited on hardly reducible ZrO<sub>2</sub> present lower activity in CO oxidation. These findings indicate the role of the support in the creation of the catalytic performance of Au nanoparticles/oxide support systems in CO oxidation. The higher reducibility suggests the presence of higher concentration of the surface oxygen vacancies, which can be the centres of the oxygen activation, as previously proposed [27]. It suggests that CO oxidation over Au/CeO<sub>2</sub> and Au/Ce<sub>0.75</sub>Zr<sub>0.25</sub>O<sub>2</sub> catalysts occurs by the reaction between CO adsorbed mostly on Au nanoparticles and oxygen that can be adsorbed and activated on the oxygen vacancies of the support surface. The oxygen vacancies can be either distant from the Au particles, in which case the active oxygen species would migrate by a spill-over towards the active Au centres with chemisorbed reactant or situated at the periphery of the Au particles [28]. However, for Au/ZrO<sub>2</sub>, the adsorption and activation of both CO and O<sub>2</sub> probably occurs on Au particles and reaction between the adsorbed CO and O species is realized by Langmuir-Hinshelwood mechanism. Therefore, we believe that the different mechanism of CO oxidation over the studied catalysts depends on the nature of the oxide support and it

is a reason for different effect of moisture on their catalytic activity.

For Au/CeO<sub>2</sub> and Au/Ce<sub>0.75</sub>Zr<sub>0.25</sub>O<sub>2</sub> catalysts, the increase in CO conversion at low moisture content (10–1000 ppm H<sub>2</sub>O) can be attributed to a change in the content of water-derived species, which may activate O<sub>2</sub> molecules, aiding their dissociation, and/or modifying the electronic state of Au at the surface [4, 29]. Next, the activated oxygen can rapidly react with CO adsorbed on the Au particles. We believe that the observed positive effect of moisture does not originate from the direct reaction of CO with water in the vapour phase to produce CO<sub>2</sub> and H<sub>2</sub> (water-gas shift reaction). According to the literature [30, 31], WGSR does occur over Au/CeO<sub>2</sub> catalysts, however the reaction temperature (300 °C) is much higher than that observed in this study. The formation of H<sub>2</sub> was also not detected. Moreover, the promoting concentration of H<sub>2</sub>O (10–1000 ppm) is significantly lower than those of CO and O<sub>2</sub> (16,000 ppm and 33,000 ppm, respectively) required by the stoichiometry of the reaction. The suppression of CO conversion at high moisture content takes place probably due to the adsorption of water on oxygen vacancies, which are blocked for the further adsorption of oxygen.

A significant effect of moisture in the reactant gas on the catalytic activity of Au/TiO<sub>2</sub> in CO oxidation was also observed by Daté and Haruta [9]. They reported that the optimal concentration of moisture for the catalytic reaction was ~200 ppm. The further increase in the concentration of moisture suppressed the catalytic activity due to the blocking of the active sites. Grunwald et al. [32] also observed similar effects of moisture on the activity of Au/TiO<sub>2</sub> in CO oxidation. They proposed that the inhibition effect of water at high moisture content is caused either by the adsorption of water on the active sites or pore filling (capillary condensation).

For Au/ZrO<sub>2</sub> catalyst, a continuous augmentation of CO conversion with the increase in the moisture content was observed. Considering that Au/ZrO<sub>2</sub> catalyst is much more resistant to the reduction than Au/Ce<sub>0.75</sub>Zr<sub>0.25</sub>O<sub>2</sub> and Au/CeO<sub>2</sub>, one can expect that the adsorption and activation of CO and O<sub>2</sub> occur on Au particles and the reaction takes place without the contribution of ZrO<sub>2</sub>. Since CO conversion increases only with a considerable amount of moisture in the gas mixture (>1000 ppm H<sub>2</sub>O), it could be suggested that its presence is necessary for the adsorption of oxygen on Au/ZrO<sub>2</sub>. Similar effect of moisture on the activity of Au/SiO<sub>2</sub> catalyst in CO oxidation was also found by Daté et al. [29].

Summarizing, the observed effect of moisture on the activity of Au/Ce<sub>1-x</sub>Zr<sub>x</sub>O<sub>2</sub> (x = 0, 0.25, 1) catalysts in the CO oxidation was different, suggesting that the reaction mechanisms depend strongly on the nature of the oxide support. Moreover, the effect of moisture was basically

reversible. For Au/CeO<sub>2</sub> and Au/Ce<sub>0.75</sub>Zr<sub>0.25</sub>O<sub>2</sub>, the optimal concentration of moisture (200–1000 ppm) leading to the significant increase in CO conversion was found. The further increase in its concentration suppressed the catalytic activity. Basing on the obtained experimental results together with those reported previously, we consider that moisture can play very significant role in the CO oxidation, especially in the activation of oxygen. The perimeter interfaces appear to act as major active sites, whereas the support surface as a moisture reservoir. On the other hand, for Au/ZrO<sub>2</sub> catalyst a continuous augmentation with the increase in the moisture content was observed. Since the reaction takes place only with the considerable amount of moisture, its presence might be indispensable for the adsorption and activation of oxygen on Au/ZrO<sub>2</sub> catalyst surface.

### 3.2.2 Effect of Pretreatment

The activity of the studied catalysts in CO oxidation also depends on the pretreatment conditions prior to the reaction. In this part of the study, the catalytic activity tests were performed at dry CO/O<sub>2</sub> gas mixture (~0.7 ppm H<sub>2</sub>O). The thermal treatment in dry He (even at temperature as low as 100 °C and/or 200 °C) suppresses their catalytic activity. The significant decrease in CO conversion (ca. 50%) at 30 °C over Au/Ce<sub>0.75</sub>Zr<sub>0.25</sub>O<sub>2</sub> and Au/CeO<sub>2</sub> catalysts was observed (Fig. 5). For Au/ZrO<sub>2</sub>, the temperature at which CO oxidation occurs was also higher. However, the loss of activity was completely restored by the exposition of the catalysts to the moisture/He stream (6000 ppm H<sub>2</sub>O) at room temperature. It suggests that the observed deactivation takes place due to the dehydroxylation of Au-OH species on the catalyst surface, as previously proposed by Costello et al. [10].

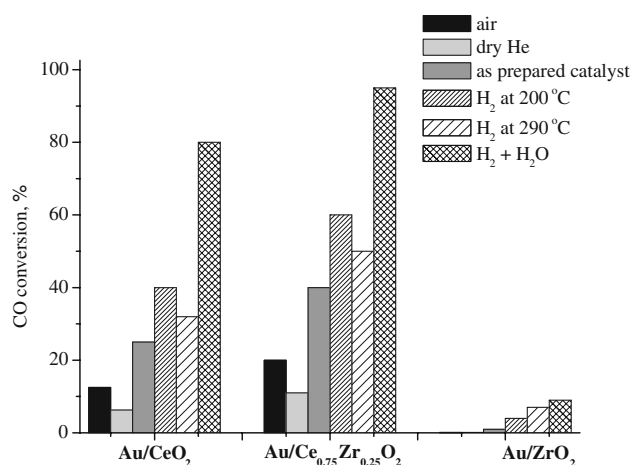


**Fig. 5** The effect of pretreatment on CO conversion at 30 °C over Au/CeO<sub>2</sub>, Au/Ce<sub>0.75</sub>Zr<sub>0.25</sub>O<sub>2</sub> and Au/ZrO<sub>2</sub> catalysts (CO:O<sub>2</sub>:He = 1.7:3.4:balance; W/F = 0.12 g s cm<sup>-3</sup>)

On the other hand, for as prepared Au/Ce-containing catalyst precursors (dried at 120 °C), tested in CO oxidation without further pretreatment, CO conversion at 30 °C is around two times higher than that for the catalysts calcined at 300 °C (Fig. 5). It is not surprising since dried samples contain some quantities of both physis- and chemisorbed water which can promote the activity at low temperature. No CO conversion was observed over dried Au/ZrO<sub>2</sub> at low temperature, similarly to the catalyst calcined at 300 °C.

The observed effects imply that the activity of the studied Au catalysts in CO oxidation depends on the amount of moisture adsorbed on the catalyst rather than on its content in the feed stream, which suggests that the reaction involves water-derived species on the catalysts surface.

The pretreatment of the studied catalysts in H<sub>2</sub> stream (pre-reduction) at different temperature led to the distinct changes in the catalysts activity in CO oxidation (Fig. 5). After the H<sub>2</sub> pre-reduction of Au/CeO<sub>2</sub> and Au/Ce<sub>0.75</sub>Zr<sub>0.25</sub>O<sub>2</sub> catalysts at 200 °C, the increase in the CO conversion from ca. 12% to 40% and from 20% to 60% was observed, respectively, comparing to samples pre-heated in air stream. However, the same catalysts pre-reduced at higher temperature (290 °C) appeared to be less active in CO oxidation than those pre-reduced at 200 °C (Fig. 5). On the other hand, the activity of the pre-reduced catalysts is still higher than that observed over the unreduced ones. It should be also noticed that the observed increase in activity was relatively stable in time (no deactivation after a few hours of reaction), independently on the applied reduction temperature. Such effect could be related to the reduction (“cleaning”) of oxide species on the surface of the Au particles rather than to the reduction of the support, as previously proposed by Ruszel et al. [27]. However, only partial pre-reduction of Au<sup>3+</sup> ions to Au<sup>0</sup> atoms (pre-reduction at lower temperature –200 °C) leads to the increase in CO conversion over Au/CeO<sub>2</sub> and Au/Ce<sub>0.75</sub>Zr<sub>0.25</sub>O<sub>2</sub> catalysts. The presence of higher amount of Au<sup>0</sup> atoms, after the reduction at higher temperature (290 °C), made those catalysts less active in CO oxidation. Those data suggest that both metallic and oxidized gold species are responsible for the catalytic oxidation of CO, as proposed by Kang and Wan [33] and Visco et al. [34]. Bond and Thompson [2] also postulated two active forms of Au: Au<sup>0</sup> which adsorbs CO, and Au (III), which joins metallic particles on the support and activates surface hydroxy groups for reaction with the adsorbed CO to form adsorbed carboxylate, responsible for high activity. Also, Fu et al. [35] proposed that Au(I)-OH and metallic gold were active for CO oxidation over Au/γ-Al<sub>2</sub>O<sub>3</sub>. On the other hand, according to Haruta [36], metallic gold particles are the active species for CO oxidation. Moreover, their presence in



very active Au/TiO<sub>2</sub> catalyst was confirmed by XPS [37]. As it could be seen, the nature of the active gold sites is still not clear, and can be determined by the nature of the oxide used as support for Au nanoparticles, the catalysts preparation method, the Au particle size, etc.

Different effect of H<sub>2</sub> pretreatment on the activity of Au/ZrO<sub>2</sub> catalyst in CO oxidation was observed. Its pre-reduction 290 °C led to the increase in CO conversion over the catalyst pre-reduced at 200 °C, contrary to Au/CeO<sub>2</sub> and Au/Ce<sub>0.75</sub>Zr<sub>0.25</sub>O<sub>2</sub> catalysts. On the other hand, it should be noticed that the reducibility of Au/ZrO<sub>2</sub> catalyst at low temperature (<300 °C) is much lower than that of Au/CeO<sub>2</sub> and/or Au/Ce<sub>0.75</sub>Zr<sub>0.25</sub>O<sub>2</sub> and that the major H<sub>2</sub> consumption for its reduction starts at temperature higher than 450 °C. It suggests that the pre-reduction of a part of Au<sup>3+</sup> ions to Au<sup>0</sup> atoms led to the increase in CO conversion, as previously proposed by Zhang et al. [38]. The same authors demonstrated that the complete reduction of all the Au<sup>3+</sup> ions would make the catalyst less active in CO oxidation.

The highest activity in CO oxidation was observed after the catalysts pretreatment in H<sub>2</sub>/H<sub>2</sub>O gas mixture (Fig. 5). It should be noticed that the pretreatment in H<sub>2</sub> was not so effective. On the other hand, CO conversion over the calcined catalysts was lower than that observed over the as-prepared catalyst precursors. Taking into consideration that during the calcination process the catalysts “autoreduction” occurs, the contrary effect should be expected. On the other hand, calcination is also accompanied by the catalysts dehydration. It suggests that the observed decrease in CO conversion could be related to the loss of hydroxyl groups during this process, confirming that the presence of metallic Au atoms on the catalysts surface is not the only condition that needs to be met to guarantee high activity in CO oxidation. However, the additional presence of H<sub>2</sub>O during the pretreatment in H<sub>2</sub> can prevent the complete reduction of Au, remaining its part in a cationic state with a hydroxyl ligand and/or change the content of water-derived species, which may activate O<sub>2</sub> molecules, aiding their dissociation. It results in the significant increase of activity. When Au nanoparticles were deposited on reducible oxide, the higher activity in CO oxidation was observed, indicating the role of the support in the creation of the catalytic performance of Au nanoparticles/oxide support systems in CO oxidation. Moreover, CO conversion over Au/CeO<sub>2</sub> and Au/Ce<sub>0.75</sub>Zr<sub>0.25</sub>O<sub>2</sub> is much higher after pretreatment in H<sub>2</sub> + H<sub>2</sub>O stream than that observed in wet conditions. It suggests that moisture can both enhance the dissociation of O<sub>2</sub> molecules adsorbed on the oxygen vacancies and modify the electronic state of gold. Next, the activated oxygen can rapidly react with CO adsorbed on the metallic Au particles. Since Au/ZrO<sub>2</sub> catalyst is much more resistant to the reduction, comparing to Au/Ce<sub>0.75</sub>Zr<sub>0.25</sub>O<sub>2</sub> and Au/CeO<sub>2</sub>,

one can expect that the reaction takes place without the contribution of ZrO<sub>2</sub>. In this case the model of the active sites for CO oxidation is an ensemble consisting of a cationic Au with a hydroxyl ligand and neighboring metallic Au atoms, as proposed by Costello et al. for Au/Al<sub>2</sub>O<sub>3</sub> [39].

As it could be seen, CO oxidation reaction over both Au/CeO<sub>2</sub> and Au/Ce<sub>0.75</sub>Zr<sub>0.25</sub>O<sub>2</sub> catalysts involves a different mechanism from that over Au/ZrO<sub>2</sub> one. Although the nature of the active sites and the reaction mechanism is still under discussion, many researchers agreed that the contact boundaries between Au and the oxide support can play a very important role in the catalytic reaction [1, 2]. Thus, the properties of the Au-oxide contacts boundaries as well as the particle size of both Au and the oxide support should be considered as important factors influencing the catalytic performance of supported Au catalysts in CO oxidation. According to Carrettin et al. [40], the higher amount of oxygen vacancies in nanosized (3–4 nm) CeO<sub>2</sub> oxide support was crucial for the activation of oxygen in the CO oxidation over Au/CeO<sub>2</sub> catalyst. The significant increase in CO conversion with the decrease in the size of ZrO<sub>2</sub> support nanoparticles was also observed over Au/ZrO<sub>2</sub> catalyst by Zhang et al. [8]. They reported that the continuous reduction in the particle size of ZrO<sub>2</sub> not only leads to the increase in Au-oxide contact boundaries in the Au/ZrO<sub>2</sub> catalyst but also modifies the chemical properties of such boundaries due to the presence of larger number of oxygen vacancies at the surface of smaller ZrO<sub>2</sub> nanoparticles which can be centers for oxygen activation. Considering that the presence of smaller particles of both Au (4–5 nm) and oxide support (4–5 nm) leads to the increase in the Au-oxide contact boundaries, the observed differences in the activities of the studied catalysts in CO oxidation are not surprising. The lowest activity was obtained over Au/ZrO<sub>2</sub> catalyst, which was characterized with the biggest particle size of both Au and the oxide support (Table 1). From that reason the lower contact boundaries between Au and ZrO<sub>2</sub> support can be expected, comparing to Au/CeO<sub>2</sub> and Au/Ce<sub>0.75</sub>Zr<sub>0.25</sub>O<sub>2</sub> catalysts. As it could be seen, the support nature (e.g. reducibility) is not the only one parameter influencing the catalytic activity of supported Au catalysts. The oxide support particle size also appears to be crucial.

## 4 Conclusions

The effect of moisture in the reactant gas on CO conversion over Au/CeO<sub>2</sub>, Au/ZrO<sub>2</sub> and Au/Ce<sub>0.75</sub>Zr<sub>0.25</sub>O<sub>2</sub> catalysts has been studied in a wide range of concentrations (~0.7–6000 ppm). Moisture generates a positive effect on catalytic activity in CO oxidation and wet conditions gave higher CO conversions. The activity is mainly affected by the amount of moisture adsorbed on the catalyst. The optimal

concentration of moisture (200–1000 ppm) for CO oxidation over Au/CeO<sub>2</sub> and Au/Ce<sub>0.75</sub>Zr<sub>0.25</sub>O<sub>2</sub> has been found. The moisture might activate O<sub>2</sub> molecules on the oxygen vacancies of the support surface and/or modify the electronic state of Au. When the moisture concentration is  $\geq 2000$  ppm, the activity is suppressed probably due to the blocking of the catalytic active sites or competitive adsorption of moisture and O<sub>2</sub>. For Au/ZrO<sub>2</sub> catalyst the presence of moisture seems to be indispensable for the oxygen adsorption on the catalyst surface. High CO conversion at room temperature over Au/Ce<sub>0.75</sub>Zr<sub>0.25</sub>O<sub>2</sub> and Au/CeO<sub>2</sub> suggests that those systems can find practical application as catalysts for pollution abatement in ambient air.

Basing on the data obtained in this study, we propose the model of the active sites for CO oxidation over the studied catalysts. In the case of Au/Ce<sub>0.75</sub>Zr<sub>0.25</sub>O<sub>2</sub> and Au/CeO<sub>2</sub> catalysts, adsorption and activation of CO takes place mostly on Au nanoparticles and adsorption and activation of O<sub>2</sub> may occur on the oxygen vacancies on the support surface. Moisture, when present, might activate O<sub>2</sub> molecules on the oxygen vacancies of the support surface and/or modify the electronic state of Au. The perimeter interfaces appear to act as major active sites, whereas the support surface as a moisture reservoir. For Au/ZrO<sub>2</sub> catalyst, adsorption and activation of CO and O<sub>2</sub> may occur on Au nanoparticles. Au (I) with a hydroxyl ligand can eventually provide the pathway for the CO conversion.

**Acknowledgments** This research was supported by Grant PBZ-KBN-116/T09/2004 (No. K124/1B/2005). The authors are grateful to Dr. Miguel Ángel Gómez García for fruitful discussions.

## References

1. Hashmi ASK, Hutchings GJ (2006) *Angew Chem Int Ed* 45:7896
2. Bond GC, Thompson DT (1999) *Catal Rev Sci Eng* 41(3–4):319
3. Dobrosz I, Jiratova K, Pitchon V, Rynkowski JM (2005) *J Mol Catal A Chem* 234:187
4. Park ED, Lee JS (1999) *J Catal* 186:1
5. Casaletto MP, Longo A, Venezia AM, Martorana A, Prestianni A (2006) *Appl Catal A* 302:309
6. Haruta M, Daté M (2001) *Appl Catal A* 222:427
7. Bond GC, Thompson DT (2000) *Gold Bull* 33:41
8. Zhang X, Wang H, Xu BQ (2005) *J Phys Chem B* 109:9678
9. Daté M, Haruta M (2001) *J Catal* 201:221
10. Costello CK, Kung MC, Oh H-S, Wang Y, Kung HH (2002) *Appl Catal A* 232:159
11. Cunningham DAH, Vogel W, Haruta M (1999) *Catal Lett* 63:43
12. Bollinger MA, Vanice MA (1996) *Appl Catal B* 8:417
13. Olea M, Tada M, Iwasawa Y (2007) *J Catal* 248:60
14. Dobrosz-Gómez I, Kocemba I, Rynkowski JM (2008) *Appl Catal B Environ* 83:240
15. Dobrosz-Gómez I, Kocemba I, Rynkowski JM, *Appl Catal B Environ* (2008) (In press)
16. Hutchings GJ (1996) *Gold Bull* 29(4):123
17. Trovarelli A (1996) *Catal Rev Sci Eng* 38:439
18. Rynkowski JM, Lewicki A, Szyrkowska MI, Paryjczak T (1999) *Chem Environ Res* 8(3&4):261
19. Concepción P, Corma A, Silvestre-Albero J, Franco V, Chan-Ching JY (2004) *J Am Chem Soc* 126:5523
20. Sun C, Li H, Chen L (2007) *J Phys Chem Solids* 68:1785
21. Shyu JZ, Weber WH, Peters CR, Usmen R (1988) *J Phys Chem* 92:4964
22. He H, Dai HX, Au CT (2004) *Catal Today* 90:245
23. Ilieva L, Sobczak JW, Manzoli JM, Su BL, Andreeva D (2005) *Appl Catal A Gen* 291:85
24. Fu Q, Saltsburg H, Flytzani-Stephanopoulos M (2003) *Science* 301:935
25. Scirè S, Minicò M, Crisafulli C, Satriano C, Pistone A (2003) *Appl Catal B Environ* 40:43
26. Trovarelli A (ed) (2002) In: *Catalysis by ceria and related materials*. ICP
27. Ruszel M, Grzybowska B, Samson K, Gressel I, Klisińska A (2006) *Catal Today* 112:126
28. Grzybowska-Świerkosz B (2006) *Catal Today* 112:3
29. Daté M, Okumura M, Tsubota S, Haruta M (2004) *Angew Chem Int Ed* 43:2129
30. Idakiev V, Tabakova T, Tenchev K, Yuan Z-Y, Ren T-Z, Su B-L (2007) *Catal Today* 128:223
31. Sandoval A, Gómez-Cortés A, Zanella R, Díaz G, Saniger JM (2007) *J Mol Catal A Chem* 278:200
32. Grunwaldt JD, Keener C, Wogerbauer C, Baiker A (1999) *J Catal* 181:223
33. Kang Y-M, Wan B-Z (1997) *Catal Today* 35:379
34. Visco AM, Neri F, Neri G, Donato A, Milone C, Galvagno SX (1999) *Phys Chem Chem Phys* 1:2869
35. Fu L, Wu NQ, Yang JH, Qu F, Johnson DL, Kung MC, Kung HH, Dravid VP (2005) *J Phys Chem Lett B* 109:3704
36. Haruta M (1997) *Catal Today* 36:153
37. Grunwaldt J-D, Maciejewski M, Becker OS, Fabrizioli P, Baiker A (1999) *J Catal* 186:458
38. Zhang X, Shi H, Xu B-Q (2007) *Catal Today* 122:330
39. Costello CK, Yang JH, Law HY, Wang Y, Lin J-N, Marks LD, Kung MC, Kung HH (2003) *Appl Catal A Gen* 243:15
40. Carrettin S, Concepción P, Corma A, López Nieto JM, Puentes VF (2004) *Angew Chem Int Ed* 43:2538